

Residual-based Stiffness Estimation in Robots with Flexible Transmissions

Fabrizio Flacco Alessandro De Luca

Abstract—We propose a novel approach for estimating the nonlinear stiffness of robot joints with flexible transmissions. Based on the definition of dynamic residual signals, we derive stiffness estimation methods that use only position and velocity measurements on the motor side and needs only the knowledge of the dynamic parameters of the motors. In particular, no extra force/torque sensing is needed. Two different strategies are considered, a model-based stiffness estimator and a black-box stiffness estimator. Both strategies consist of two stages. The first stage of the model-based estimator generates a residual signal that is a first-order filtered version of the flexibility torque of the transmission, while in the second stage a least squares fitting method is used to estimate the model parameters of the stiffness. The black-box estimator uses in the first stage a second-order residual that is directly a filtered version of the stiffness multiplied by the deformation rate of the transmission. In the second stage, a simple regressor provides the transmission stiffness in a singularity-robust way. Numerical results reported for the cases of constant, nonlinear, or variable stiffness transmissions demonstrate the effectiveness of the approach and the relative merits of the two estimation strategies.

I. INTRODUCTION

The current trend in lightweight robots intended for physical Human-Robot Interaction (pHRI) is to use compliant transmissions at the joints to milden the effects of possible undesired collisions. The transmissions connecting the motors to the driven links may be flexible in the linear domain (elastic), display nonlinear deformation-torque characteristics, or be part of a nonlinear variable stiffness actuation (VSA) system.

Typically, both conventional and advanced control laws for robots with flexible joints need an accurate knowledge of the joint stiffness, or at least of the flexibility (spring) torque of the transmission. In fact, for manipulators with elastic joints moving under gravity, PD control laws with different forms of gravity compensation [1], [2] use the actual joint stiffness for defining the correct reference position of the motors. A similar need arises in PD regulation under gravity of the two motor positions in the VSA-II system [3]. Even more critical are the requirements for nonlinear control laws based on feedback linearization of compliant joint robots. For instance, the simultaneous motion/stiffness decoupling control law proposed in [4] for antagonistic VSA-based manipulators involves the transmission stiffnesses, as well as their first and second derivatives with respect to joint deformation.

The authors are with the Dipartimento di Informatica e Sistemistica, Università di Roma “La Sapienza”, Via Ariosto 25, 00185 Rome, Italy {fflacco,deluca}@dis.uniroma1.it).

Unfortunately, no sensor is available for a direct measure of the transmission stiffness. Therefore, all control laws for robots with flexible transmissions gather the stiffness information by combining an accurate model of the flexibility torque, static calibration methods, as well as position and/or joint torque sensor measures. This procedure is particularly critical for VSA-based manipulators, since the transmission stiffness in this case is intrinsically nonlinear (and possibly time-varying) and the flexibility torque model may be a complex (and uncertain) function of the joint deformation.

As a result, the problem of an accurate on-line estimation of transmission stiffness appears to be crucial for control performance in pHRI tasks. While many papers have dealt with stiffness estimation [5]–[8] in the contact between the end-effector of a rigid robot and the environment/human, very few works are available on the estimation of variable, nonlinear stiffness of single or double actuated flexible joints. Grioli and Bicchi [9] have proposed a stiffness estimator based on the measure of the flexibility torque using a joint torque sensor. Their estimation process utilizes also the time derivative of the measured torque, which gives rise to problems with noisy measurements. In the latest works [10], [11], the more general problem of impedance estimation is considered and experimental results are presented for the AwAS, a variable stiffness device developed at IIT [12].

In this paper, we propose a novel approach to estimate the stiffness of a transmission proceeding along similar lines of [9]. However, our stiffness estimators need only measures of the position and velocity on the motor side of the transmission(s), together with the knowledge of the basic dynamic parameters of the motor(s). No joint torque sensing is required and the presence or absence of external torques (e.g., gravity or contact forces) acting on the link side is irrelevant. This result is obtained thanks to the use of so-called *dynamic residuals*, which are computable signals that provide filtered versions of unmeasurable/unknown dynamic terms in the system. Residuals have been used already in robotic applications for the detection of generic actuator faults [13], for model-free motor friction compensation [14], and for sensor-less collision detection and reaction [4], [15].

Two different strategies will be considered for estimating the stiffness, a model-based estimator (MBE) and a black-box estimator (BBE). Both strategies consist of two stages. The MBE uses in the first stage a residual that provides a first-order filtered version of the flexibility torque of the transmission and in the second stage a least squares algorithm that estimates the parameters of the stiffness model. This strategy can be implemented either off line or on line. On

the other hand, the BBE uses in the first stage a second-order residual that is a filtered version of the stiffness multiplied by the transmission deformation rate. In the second stage, a simple regressor provides the transmission stiffness without being affected by a singularity when the rate of joint deformation vanishes. The BBE strategy is intended for on-line application only.

The paper is organized as follows. In Sect. II we introduce the modeling framework. The MBE strategy is presented in Sect. III. In particular, the residual design for estimating the flexibility torque is given in Sect. III-A and this result is used in Sect. III-B for estimating the parameters of the transmission stiffness model using linear or nonlinear least squares techniques. The BBE strategy is presented in Sect. IV, first defining the second-order residual for the stiffness (Sect. IV-A) and then the singularity-free regressor (Sect. IV-B). Numerical simulations are reported in Sect. V for three case studies, having constant, nonlinear, or variable stiffness, to illustrate the performance of the proposed stiffness estimation strategies in unperturbed conditions. The results are discussed in the concluding Sect. VI, together with on-going and future research.

II. MODELING

We consider a flexible transmission that connects a driving motor to a driven link. The deformation $\phi = q - \theta$ of the transmission is the difference between the link position q and the motor position θ . A smooth potential function $U_e(\phi) \geq 0$, with $U_e(\phi) = 0$ iff $\phi = 0$, is associated to the deformation. The *flexibility torque* of the transmission is obtained as

$$\tau_e(\phi) = \frac{\partial U_e(\phi)}{\partial \phi}, \quad (1)$$

where we assume that

$$\tau_e(0) = 0, \quad \tau_e(-\phi) = -\tau_e(\phi), \quad \forall \phi. \quad (2)$$

The *stiffness* of the transmission is defined as the variation rate of the flexibility torque $\tau_e(\phi)$ w.r.t. the deformation ϕ ,

$$\sigma(\phi) = \frac{\partial \tau_e(\phi)}{\partial \phi} = \frac{\partial^2 U_e(\phi)}{\partial \phi^2} > 0. \quad (3)$$

For a single motor driving a rigid link subject to gravity through a (nonlinear) flexible transmission, the dynamic model takes the form

$$M\ddot{q} + D_q\dot{q} + \tau_e(\phi) + g(q) = \tau_k \quad (4)$$

$$B\ddot{\theta} + D_\theta\dot{\theta} - \tau_e(\phi) = \tau, \quad (5)$$

where $M > 0$ and $B > 0$ are the link and motor inertias, $D_q \geq 0$ and $D_\theta \geq 0$ are viscous friction coefficients at the two sides of the transmission, τ is the control torque produced by the motor, and $g(q)$ and τ_k are, respectively, the gravity and further environment/disturbance torques acting on the link.

In robot joints with variable stiffness actuation (VSA) two motors, either in antagonist or in serial configuration, are connected to the driven link through possibly *different* linear or nonlinear flexible transmissions (including Harmonic

Drives) and nonlinear kinematics structures. The model becomes

$$M\ddot{q} + D_q\dot{q} + \tau_{e,t}(\phi) + g(q) = \tau_k \quad (6)$$

$$B_i\ddot{\theta}_i + D_{\theta,i}\dot{\theta}_i - \tau_{e,i}(\phi_i) = \tau_i, \quad i = 1, 2. \quad (7)$$

With a slight abuse of notation, this model covers different realizations of the VSA concept, see, e.g., [12], [16]–[18].

The *total flexibility torque* $\tau_{e,t}$ in the link dynamics (6) is a function of $\phi = (\phi_1 \ \phi_2)^T$, the vector of transmission deformations $\phi_i = q - \theta_i$. This torque is a known (kinematic) function of the flexibility torques $\tau_{e,i}(\phi_i)$, $i = 1, 2$, usually with a separable structure. The *total stiffness* of the device is then

$$\sigma_t(\phi) = \frac{\partial \tau_{e,t}(\phi)}{\partial q} > 0. \quad (8)$$

In particular, in VSA using an antagonistic configuration of the two motors it is

$$\tau_{e,t}(\phi) = \tau_{e,1}(\phi_1) + \tau_{e,2}(\phi_2). \quad (9)$$

Accordingly, the stiffness of each transmission is

$$\sigma_i(\phi_i) = \frac{\partial \tau_{e,i}(\phi_i)}{\partial \phi_i} = \frac{\partial \tau_{e,i}(\phi_i)}{\partial q} > 0, \quad i = 1, 2, \quad (10)$$

and the total stiffness of the device is simply

$$\sigma_t(\phi) = \sigma_1(\phi_1) + \sigma_2(\phi_2). \quad (11)$$

In the following, our main goal will be to estimate the stiffness σ_i of the single transmission(s), and then the total stiffness σ_t of the device.

III. MODEL-BASED ESTIMATION OF STIFFNESS

A. Residual for flexibility torque estimation

In the first stage of the MBE strategy, we estimate the flexibility torque τ_e associated to a transmission (or the $\tau_{e,t}$ of the full device) by designing a *residual* signal that provides a filtered version of this unknown (or uncertain) and unmeasured quantity. For this problem, one can follow in principle two different modes that we call *external* and *internal*, respectively.

In the external mode, with reference to eq. (6) of a VSA system, we use $p_q = M\dot{q}$, the generalized momentum of the link, and define the residual as

$$r_{\tau_{e,t}} = K_{\tau_{e,t}} \left(p_q + D_q q - \int_0^t (\tau_k - g(q) + r_{\tau_{e,t}}) dt_1 \right), \quad (12)$$

where $K_{\tau_{e,t}} > 0$ is a free design parameter. It is easy to see that the residual (12) will evolve as

$$\dot{r}_{\tau_{e,t}} = K_{\tau_{e,t}} (-\tau_{e,t}(\phi) - r_{\tau_{e,t}}), \quad (13)$$

resulting in a stable, first-order filtered version of $-\tau_{e,t}$. Indeed, an equivalent scheme can be set up also for estimating τ_e in the single transmission case of eq. (4). While eq. (12) nicely provides an estimate of the total flexibility torque of the device, it needs the knowledge of the nonlinear gravity term and, most critically, also the knowledge or a measure by a torque sensor of the environment/disturbance torque

τ_k . Moreover, it is in general impossible to decompose the estimate of $\tau_{e,t}$ into its single components estimating each $\tau_{e,i}$ —see eq. (9).

In presenting the internal mode, we will omit the subscript i when referring to each transmission of a VSA system, i.e., to eq. (7), since the residual will be identical to the case of a single transmission (see eq. (5)). In this case, we use the generalized momentum of the motor $p_\theta = B\dot{\theta}$ and define the residual as

$$r_{\tau_e} = K_{\tau_e} \left(p_\theta + D_\theta \theta - \int_0^t (\tau + r_{\tau_e}) dt_1 \right), \quad (14)$$

where $K_{\tau_e} > 0$ is again a design parameter. The residual r_{τ_e} satisfies

$$\dot{r}_{\tau_e} = K_{\tau_e} (\tau_e - r_{\tau_e}), \quad (15)$$

resulting again in a stable, first-order filter of the unknown flexible torque τ_e . In the Laplace domain, we rewrite (15) as

$$\frac{r_{\tau_e}(s)}{\tau_e(s)} = \frac{K_{\tau_e}}{s + K_{\tau_e}}. \quad (16)$$

As opposed to the residual (12), the evaluation of r_{τ_e} involves only the motor variables θ and $\dot{\theta}$, as well as the known control torque τ . Note that the estimation capability of r_{τ_e} is rather independent from the applied control torque, which can be either an open-loop command or a feedback law (in particular, one that uses the estimate itself). In the VSA case, once an independent residual (14) is designed for each transmission, we can combine the two estimates $r_{\tau_{e,1}}$ and $r_{\tau_{e,2}}$ in the same way as we combine the true values $\tau_{e,1}$ and $\tau_{e,2}$ (see, e.g., eq. (9) for the simple antagonistic case) and obtain an estimate of the total flexibility torque. As a result, the internal mode of residual generation seems preferable.

B. Least squares estimation of stiffness

Using the internal residual of Sect. III-A as an estimate of the transmission flexibility torque τ_e , the model-based estimator (MBE) for the stiffness σ can be set up assuming that a parametric model of the functional dependence of τ_e on ϕ is available. In general, this will be a *nonlinear* function of a n -vector of constant parameters $\alpha = (\alpha_1 \dots \alpha_n)^T$,

$$\tau_e(\phi) = f(\phi, \alpha). \quad (17)$$

If α were known, the stiffness could be computed from (3) and (17) as

$$\sigma(\phi) = \frac{\partial f(\phi, \alpha)}{\partial \phi}. \quad (18)$$

As an example, consider one of the two transmissions of the VSA-II system [16]. The functional form of τ_e is

$$\tau_e(\phi) = 2k\beta(\phi) \frac{\partial \beta(\phi)}{\partial \phi}, \quad (19)$$

where k is the constant stiffness of the two springs in the transmission and

$$\beta(\phi) = \arcsin \left(C \sin \left(\frac{\phi}{2} \right) \right) - \frac{\phi}{2}, \quad (20)$$

being $C > 1$ a geometric parameter of the internal 4-bar mechanism. This model is nonlinear both in ϕ and in the uncertain parameter vector $\alpha = (k \ C)^T$ ($n = 2$).

In some special cases, the model (17) is known to be *linear* in the parameters α , i.e.,

$$f(\phi, \alpha) = \sum_{h=1}^n f_h(\phi) \alpha_h = \mathbf{F}^T(\phi) \alpha. \quad (21)$$

In general, a model of the form (21) can be chosen to approximate the actual functional form of $\tau_e(\phi)$, using suitable basis functions $f_h(\phi)$ (e.g., polynomials).

In the following, we sketch an estimation algorithm based on the standard least squares (LS) method, which will be one shot for the linearly parametrized model (21) or iterative for the nonlinear model (17). For simplicity, we present a batch (or off-line) version, although it is relatively easy to convert the LS algorithm to an on-line scheme.

Let s data points $(\phi(j), r_{\tau_e}(j))$, with $j = 1, \dots, s$ be available from a robot motion experiment, with $s \gg n$. Each data point embodies the transmission deformation and the residual estimating the flexibility torque.

In the linear case, define

$$\mathbf{J} = \begin{pmatrix} \mathbf{F}^T(\phi(1)) \\ \vdots \\ \mathbf{F}^T(\phi(s)) \end{pmatrix}, \quad \mathbf{r}_e = \begin{pmatrix} r_{\tau_e}(1) \\ \vdots \\ r_{\tau_e}(s) \end{pmatrix},$$

respectively, a $s \times n$ matrix and a s -vector. We obtain the over-constrained linear system

$$\mathbf{J} \alpha = \mathbf{r}_e \quad (22)$$

whose solution by the LS method¹ gives as estimate of α

$$\hat{\alpha} = \mathbf{J}^\# \mathbf{r}_e = \left(\mathbf{J}^T \mathbf{J} \right)^{-1} \mathbf{J}^T \mathbf{r}_e. \quad (23)$$

When the linearly parametrized model (21) is used as an approximation of the nonlinear model (17), it is convenient to resort to solutions with an increasing number p of coefficients. Taking into account the physical assumption (2) for the flexibility torque, we choose as basis functions in (21) only *odd* powers of ϕ up to the order $2p - 1$, i.e.,

$$f_h(\phi) = \phi^{2h-1}, \quad h = 1, \dots, p. \quad (24)$$

The first solution $\hat{\alpha}^{(1)}$ is obtained using only the first element ($p = 1$) of this polynomial approximation and applying eq. (23). At a generic step p , the (squared) estimation error with $\hat{\alpha}^{(p)}$ is evaluated as

$$e^{(p)} = \sum_{j=1}^s \left(r_{\tau_e}(s) - \sum_{h=1}^n f_h(\phi(s)) \hat{\alpha}_h^{(p)} \right)^2.$$

If $|e^{(p)} - e^{(p-1)}| < \gamma$, for a given small threshold $\gamma > 0$, the algorithm stops having reached a sufficient approximation. Otherwise, a polynomial model with $p = p + 1$ is taken and the process is repeated.

¹The explicit expression of the pseudoinverse on the right-hand side is valid for a full column rank matrix \mathbf{J} . In practice, replacing the inverse of matrix $\mathbf{J}^T \mathbf{J}$ with its pseudoinverse provides better results.

For the nonlinearly parametrized model (17), the iterative LS algorithm proceeds as follows. From the current estimate $\alpha^{(k)}$ at iteration k of the true parameter vector α , the new estimate is obtained as

$$\hat{\alpha}^{(k+1)} = \hat{\alpha}^{(k)} + \Delta\alpha.$$

where $\Delta\alpha$ is the vector of parameter estimation updates. Let

$$\Delta r_{\tau_e}(j) = r_{\tau_e}(j) - f(\phi(j), \hat{\alpha}^{(k)}), \quad j = 1, \dots, s,$$

and the model Jacobians

$$\mathbf{J}(j) = \left(\frac{\partial f(\phi(j), \alpha)}{\partial \alpha_1}, \dots, \frac{\partial f(\phi(j), \alpha)}{\partial \alpha_n} \right)_{\alpha = \hat{\alpha}^{(k)}},$$

for $j = 1, \dots, s$. Defining

$$\mathbf{J} = \begin{pmatrix} \mathbf{J}(1) \\ \vdots \\ \mathbf{J}(s) \end{pmatrix}, \quad \Delta \mathbf{r}_e = \begin{pmatrix} \Delta r_{\tau_e}(1) \\ \vdots \\ \Delta r_{\tau_e}(s) \end{pmatrix},$$

we obtain a linear system similar to (22)

$$\mathbf{J}\Delta\alpha = \Delta\mathbf{r}_e \quad (25)$$

having the least squares solution

$$\Delta\alpha = \mathbf{J}^\# \Delta\mathbf{r}_e. \quad (26)$$

The iteration is repeated for $k = k + 1$ until $\Delta\alpha$ is smaller in norm than a convergence tolerance $\delta > 0$.

Once a good parametric estimate $\hat{\alpha}$ has been obtained, the transmission stiffness σ is finally estimated using symbolic derivation of the identified flexibility torque model, or

$$\hat{\sigma}(\phi) = \frac{\partial f(\phi, \hat{\alpha})}{\partial \dot{\phi}}. \quad (27)$$

This completes the second stage of the MBE strategy.

IV. BLACK-BOX ESTIMATION OF STIFFNESS

A. Residual for stiffness estimation

We turn to the design of an alternative residual-based approach that provides a more direct estimate of the transmission stiffness, does not need a model of the flexible transmission torque, and works efficiently on line. To this purpose, in the first stage of the BBE strategy we introduce the following second-order residual (in internal mode)

$$r_\sigma = K_{\sigma,1} \left(p_\theta + D_\theta \theta - \int_0^t \left(\tau + \int_0^{t_1} r_\sigma dt_2 \right) dt_1 \right) - K_{\sigma,2} \int_0^t r_\sigma dt_1, \quad (28)$$

where $K_{\sigma,1} > 0$ and $K_{\sigma,2} > 0$ are two design parameters. The first time derivative of residual (28) is

$$\dot{r}_\sigma = K_{\sigma,1} \left(\dot{p}_\theta + D_\theta \dot{\theta} - \tau - \int_0^t r_\sigma dt_1 \right) - K_{\sigma,2} r_\sigma.$$

Taking into account that time differentiation of eq. (5) yields

$$B\ddot{\theta} + D_\theta \dot{\theta} = \dot{\tau}_e(\phi) + \dot{\tau}$$

and using the relation

$$\dot{\tau}_e(\phi) = \frac{\partial \tau_e(\phi)}{\partial \dot{\phi}} \dot{\phi} = \sigma(\phi) \dot{\phi}$$

obtained from the definition (3), it can be easily shown that r_σ satisfies the following second-order dynamics,

$$\ddot{r}_\sigma = K_{\sigma,1} (\sigma(\phi) \dot{\phi} - r_\sigma) - K_{\sigma,2} \dot{r}_\sigma, \quad (29)$$

that represents a stable, second-order filter driven by the unknown signal $\sigma(\phi) \dot{\phi}$. In the Laplace domain, we can rewrite (29) as

$$\frac{r_\sigma(s)}{[\sigma(\phi) \dot{\phi}](s)} = \frac{K_{\sigma,1}}{s^2 + K_{\sigma,2}s + K_{\sigma,1}}. \quad (30)$$

Increasing the gain $K_{\sigma,1}$ speeds up convergence of r_σ to $\sigma(\phi) \dot{\phi}$, while the presence of gain $K_{\sigma,2}$ is needed for asymptotic stability. It should be noted that only θ , $\dot{\theta}$, and τ are needed to compute r_σ .

B. Regressor for singularity-free stiffness estimation

Using the convergence properties shown for the second-order residual r_σ , a simple but naive way to extract an estimate $\hat{\sigma}$ of the true stiffness σ from r_σ would be to divide it by $\dot{\phi}$, or

$$\sigma(\phi) \simeq \hat{\sigma}(\phi) = \frac{r_\sigma}{\dot{\phi}}. \quad (31)$$

Obviously, there is a singularity at $\dot{\phi} = 0$ and large degradations of the estimate occur when changes in transmission deformation tends to vanish. Stated differently, in order to have a chance for a good estimation of the transmission stiffness, there is a need of a relative motion between the motor position θ and the link position q . This is also consistent with the general considerations made in [9].

To extract a stiffness estimate from the residual r_σ , while avoiding singularity or ill-conditioning, the black-box stiffness estimator is completed in the second stage by the following regressor (written in its discretized form at $t = kT$, for a given sampling interval T)

$$\begin{aligned} \hat{\sigma}(k+1) &= \hat{\sigma}(k) + K_R (r_\sigma(k) \dot{\phi}(k) - \hat{\sigma}(k) \dot{\phi}^2(k)) \\ &\simeq \hat{\sigma}(k) + K_R \dot{\phi}^2(k) (\sigma(\phi(k)) - \hat{\sigma}(k)) \\ &= (1 - K_R \dot{\phi}^2(k)) \hat{\sigma}(k) + \sigma(\phi) K_R \dot{\phi}^2(k), \end{aligned} \quad (32)$$

where $K_R > 0$. The product $K_R \dot{\phi}^2 \geq 0$ will weight the possible convergence (in time) of the stiffness estimate $\hat{\sigma}$ to the true stiffness. The gain K_R by itself can be considered as the bandwidth of a lowpass filter. Using a relatively high gain allows to track fast variation of stiffness, but the estimator will be very sensitive to noise especially at low $|\dot{\phi}|$. Conversely, a relatively low gain will filter bad estimations but also high dynamical stiffness variations. In any event, for the asymptotic stability of the discrete-time regressor (32) it is necessary that

$$|1 - K_R \dot{\phi}^2(k)| < 1 \quad \Rightarrow \quad K_R \dot{\phi}^2(k) \in [0, 2].$$

Since this condition is time-varying, a fixed choice for K_R may not always guarantee convergence of the estimation process. To overcome this problem, we use a stability recovery scheme that dynamically saturates K_R when its product by $\dot{\phi}^2(k)$ becomes too large (and thus for $|\dot{\phi}|$ certainly not close to zero). For a given $K_{max} < 2$, we set:

$$\text{if } K_R \dot{\phi}^2(k) > K_{max} \Rightarrow K_R = \frac{K_{max}}{\dot{\phi}^2(k)}. \quad (33)$$

V. NUMERICAL RESULTS

We illustrate the performance of the proposed estimation strategies on three examples of systems with different transmission flexibilities.

A. Constant stiffness

In this first example, an elastic joint with unknown but constant stiffness was considered. The dynamic model is given by eqs. (4–5), with $\tau_e(\phi) = K\phi$ and $\sigma = K$. An open-loop torque $\tau = 10 \cdot \sin 0.1\pi t$ N·mm was applied for 10 s to. The data are: $K = 100$ N·mm/rad, $B = 50$ kg·m·mm, $M = 100$ kg·m·mm, $D_\theta = 1$ N·mm·s/rad, $D_q = 0.1$ N·mm·s/rad, $g(q) = 25 \cdot \sin q$ N·mm. A Runge-Kutta routine with fixed 1 ms step was used for numerical integration.

Figure 1 shows the flexibility torque estimated using the first-order residual in eq. (14) with filter constant $K_{\tau_e} = 300$. Based on these estimated values, the MBE strategy was run on a batch of $s = 10^4$ data points collected over 10 s, using a polynomial model as in (21) and (24). Using as threshold $\gamma = 10^{-2}$, the LS algorithm with polynomials of increasing order stops, as one could expect, at the first iteration ($p = 1$), giving the stiffness estimate $\hat{\alpha}_1 = \hat{K} = 99.997$ N·mm/rad.

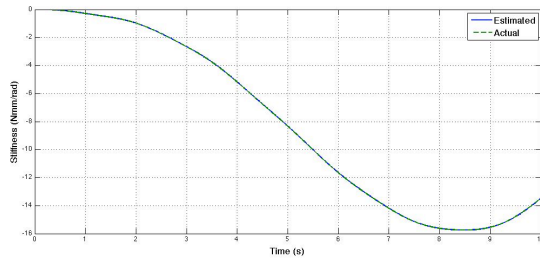


Fig. 1. Flexibility torque τ_e for an elastic joint estimated during forced motion using the residual (14)

Figure 2 shows the on-line stiffness estimation obtained with the BBE strategy, using the second-order residual in eq. (28) with filter constants $K_{\sigma,1} = 300$ and $K_{\sigma,2} = 1$, and a constant regressor gain $K_R = 1900$ in eq. (32) without the stability recovery scheme. The initial estimate \hat{K} was set to 0. As soon as the product $K_R \dot{\phi}^2$ becomes larger than 2, the algorithm becomes unstable. Figure 3 shows the improved behavior of the estimated stiffness when introducing the stability recovery scheme (33), with $K_{max} = 1.9$.

B. Quadratic stiffness

In the second example, we have considered a nonlinear transmission with cubic characteristic for the flexibility

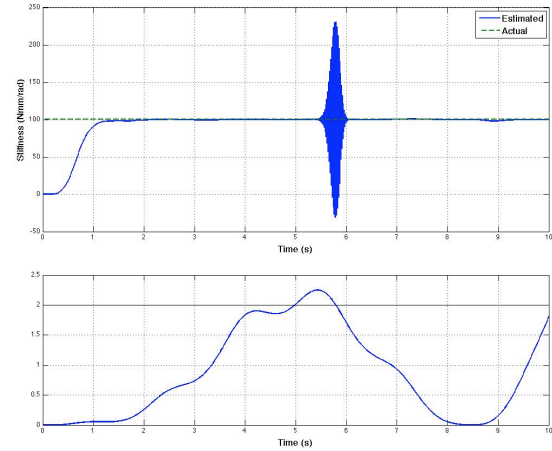


Fig. 2. On-line stiffness estimation for an elastic joint using the BBE strategy without the stability recovery scheme (top) and evolution of the dimensionless product $K_R \dot{\phi}^2$ (bottom)

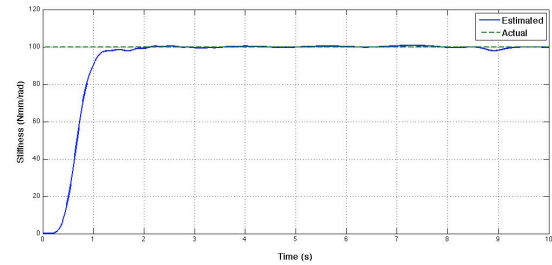


Fig. 3. On-line stiffness estimation for an elastic joint using the BBE strategy with the stability recovery scheme (33)

torque (quadratic stiffness),

$$\tau_e(\phi) = K_1\phi + K_3\phi^3, \quad (34)$$

with $K_1 = 100$ N·mm/rad and $K_3 = 500$ N·mm/rad. All other model parameters and the applied torque τ were chosen as in the previous example.

Figure 4 shows the flexibility torque estimated using the first-order residual in eq. (14) with $K_{\tau_e} = 300$. The MBE strategy for stiffness estimation was applied in exactly the same operative conditions of Sect. V-A. The LS algorithm with polynomials of increasing order stops in this case at $p = 2$, yielding $\hat{\alpha}_1 = \hat{K}_1 = 99.997$ and $\hat{\alpha}_2 = \hat{K}_3 = 501.71$, in good agreement with the nominal data. Accordingly, the quadratic stiffness is estimated as $\hat{\sigma}(\phi) = \hat{K}_1 + 3\hat{K}_3\phi^2$.

The on-line stiffness estimation obtained with the BBE strategy using the second-order residual in eq. (28) is shown in Fig. 5. Estimation gains were as in the previous example.

C. Nonlinear stiffness of the VSA-II

As a last example, we have considered the VSA-II device of the University of Pisa [16], where two motors in antagonistic configuration drive a single link under gravity via two transmissions, each having a nonlinear torque-deformation characteristic of the form (19–20). The total flexibility torque acting on the link dynamics is given by the sum in eq. (9).

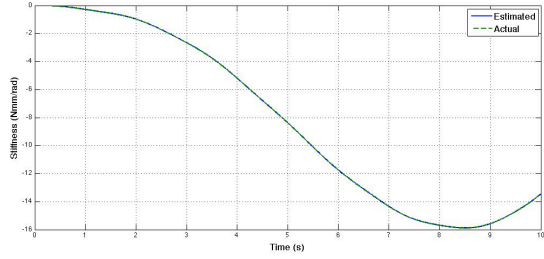


Fig. 4. Flexibility torque τ_e for a joint with quadratic stiffness estimated during forced motion using the residual (14)

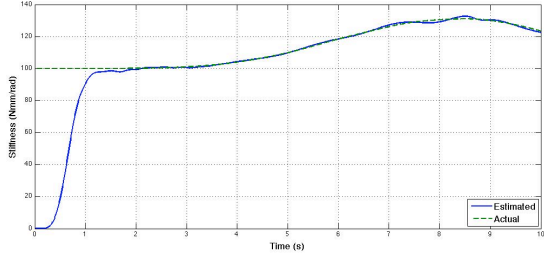


Fig. 5. On-line stiffness estimation for a joint with quadratic stiffness using the BBE strategy with the stability recovery scheme (33)

We have used the data of the VSA-II reported in [16]. In particular, the values of the two parameters that characterize the flexible transmissions are $k_i = 500$ N·mm/rad and $C_i = 1.75$, for both $i = 1, 2$. Two open-loop torques $\tau_1 = 10 \cdot \sin 0.1\pi$ N·mm and $\tau_2 = 10 \cdot \sin 0.2\pi$ N·mm were applied for 10 s.

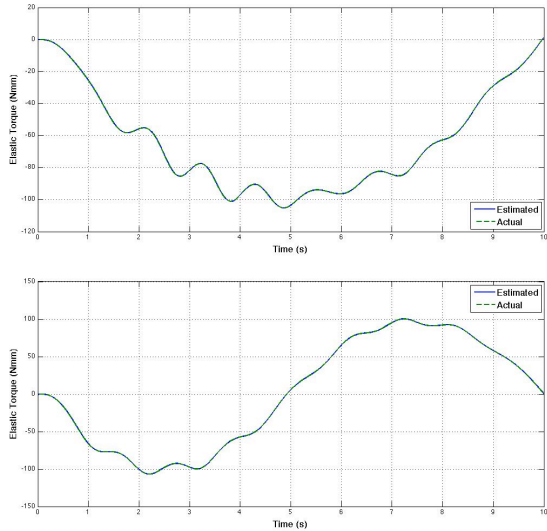


Fig. 6. Flexibility torques $\tau_{e,1}$ (top) and $\tau_{e,2}$ (bottom) for the VSA-II estimated during forced motion using two residuals as in eq. (14)

Using two first-order residuals as in eq. (14), both with equal $K_{\tau_e} = 300$, we obtain the estimation of the two flexibility torques of the VSA-II shown in Fig. 6. Based on these estimated values, the MBE strategy for estimating the stiffness of the VSA-II has been implemented in two

versions, either using approximating polynomial models for the two nonlinear flexibility torques or considering the transmission model (19–20) with the parameters appearing in a nonlinear way.

In the first case, using $s = 10^5$ data points and a threshold $\gamma = 10^{-2}$, the LS algorithm with polynomials of increasing order stops at $p = 5$, providing for the first transmission

$$\hat{\alpha} = (140.623, 112.805, 73.184, 43.548, 41.891)^T,$$

and for the second transmission

$$\hat{\alpha} = (140.628, 112.698, 73.94, 41.71, 43.086)^T.$$

Figure 7 shows a comparison of the actual stiffness profiles of the two VSA-II transmissions with those estimated using the MBE strategy with polynomial approximation.

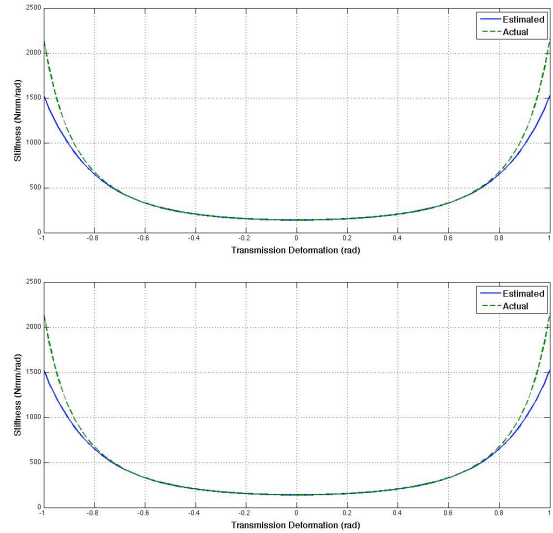


Fig. 7. Comparison of actual and estimated stiffness characteristics for transmission 1 (top) and 2 (bottom) of the VSA-II when using with the polynomial MBE strategy

Using instead the MBE strategy with the nonlinearly parametrized model, the iterative LS algorithm reached convergence (with $\delta = 1$) after $k = 55$ and $k = 32$ iterations, respectively for the first and second transmission. The common initialization of the two pairs of parameter estimates was $\hat{k}_i = 100$ and $\hat{C}_i = 1.1$, for $i = 1, 2$. The obtained final values are:

$$\hat{k}_1 = 499.22, \quad \hat{C}_1 = 1.7536, \quad \hat{k}_2 = 499.96, \quad \hat{C}_2 = 1.7527.$$

Figure 8 shows the on-line stiffness estimation for the two transmissions obtained with the BBE strategy, using two second-order residuals as in eq. (28) with $K_{\sigma,1} = 5000$ and $K_{\sigma,2} = 1$, and a regressor gain $K_R = 1$ in eq. (32). The initial estimates were all set to 0. The resulting on-line estimation of the total stiffness of the VSA-II device is shown in Fig. 9.

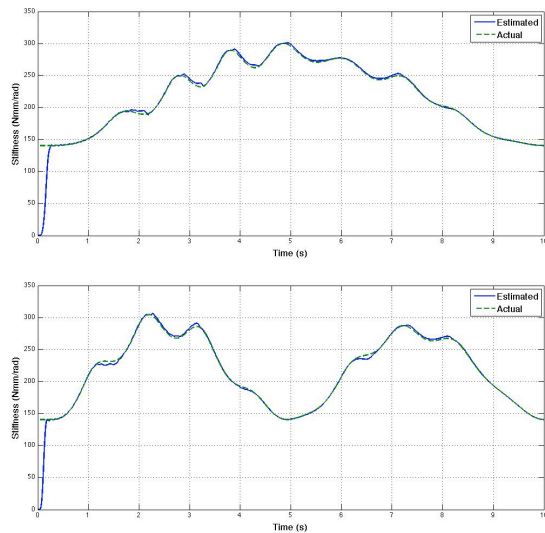


Fig. 8. On-line stiffness estimation for transmissions 1 (top) and 2 (bottom) of the VSA-II using the BBE strategy and the stability recovery scheme (33)

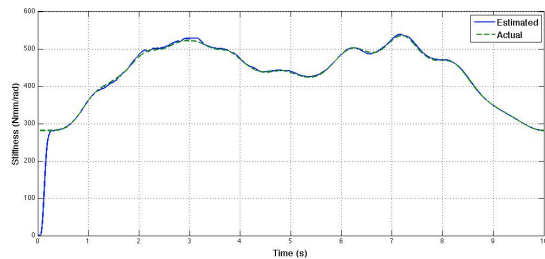


Fig. 9. On-line estimation of the *total* stiffness of the VSA-II device resulting from Fig. 8

VI. CONCLUSIONS

The two presented MBE (model-based) and BBE (black-box) strategies for estimating transmission stiffness have the same working conditions. Only measures of position/velocity of the motors and knowledge of their inertia and viscous damping are assumed to be available. Thanks to the use of dynamic residuals, joint torque sensing is never required.

Although the MBE strategy has been applied here only with batch processing of measured data and generated residuals, its on line implementation with a recursive weighted LS has been also developed. In off-line batch processing, the iterative least squares algorithm appears to be slow for a nonlinearly parameterized stiffness model, while using linear parameterizations of increasing order is considerably faster.

The MBE strategy is to be preferred when the estimation process is intended for real-time control. Having a stiffness model with identified parameters allows its symbolic differentiation for obtaining the terms needed in feedback linearization control. Moreover, since MBE is based on first-order residuals, its discrete-time implementation is easier to tune and introduces only a single step delay. On the other hand, BBE is an attractive estimation strategy since it does not rely on a specific stiffness model. In particular, BBE

copies well also with the possible time-varying nature of the stiffness characteristics of a transmission.

We are currently extending our stiffness estimation approach to variable stiffness with serial actuation, and also verifying the performance when using estimated rather than nominal stiffness data in feedback control laws. In forthcoming experiments, we shall test the sensitivity of the approach to sensor noise, discrete-time implementation, uncertain motor inertia or viscous damping, and unmodeled friction.

REFERENCES

- [1] P. Tomei, "A simple PD controller for robots with elastic joints," *IEEE Trans. on Automatic Control*, vol. 36, no. 10, pp. 1208–1213, 1991.
- [2] A. Kugi, C. Ott, A. Albu-Schäffer, and G. Hirzinger, "On the passivity-based impedance control of flexible joint robots," *IEEE Trans. on Robotics*, vol. 24, no. 2, pp. 416–429, 2008.
- [3] G. Tonietti, R. Schiavi, and A. Bicchi, "Design and control of a variable stiffness actuator for safe and fast physical human/robot interaction," in *Proc. IEEE Int. Conf. on Robotics and Automation*, 2005, pp. 528–533.
- [4] A. De Luca, F. Flacco, A. Bicchi, and R. Schiavi, "Nonlinear decoupled motion-stiffness control and collision detection/reaction for the VSA-II variable stiffness device," in *Proc. IEEE/RSJ Int. Conf. on Intelligent Robots and Systems*, 2009, pp. 5487–5494.
- [5] N. Diolaiti, C. Melchiorri, and S. Stramigioli, "Contact impedance estimation for robotic systems," *IEEE Trans. on Robotics*, vol. 21, no. 5, pp. 925–935, 2005.
- [6] D. Verschuere, I. Scharf, H. Bruyninckx, J. Swevers, and J. De Schutter, "Identification of contact dynamics parameters for stiff robotic payloads," *IEEE Trans. on Robotics*, vol. 25, no. 2, pp. 240–252, 2009.
- [7] F. Coutinho and R. Cortesao, "System stiffness estimation with the candidate observers algorithm," in *Proc. 18th Mediterranean Conf. on Control and Automation*, 2010, pp. 796–801.
- [8] D. Ludvig and R. E. Kearney, "Estimation of joint stiffness with a compliant load," in *Proc. 31st IEEE Int. Conf. on EMBS*, 2009, pp. 2967–2970.
- [9] G. Grioli and A. Bicchi, "A non-invasive real-time method for measuring variable stiffness," in *Proc. Robotics Science and Systems (RSS 2010)*, Zaragoza, E, 2010.
- [10] A. Serio, G. Grioli, I. Sardellitti, N. G. Tsagarakis, and A. Bicchi, "A decoupled impedance observer for a variable stiffness robot," in *Proc. IEEE Int. Conf. on Robotics and Automation*, Shanghai, PRC, 2011 (this conference).
- [11] G. Grioli and A. Bicchi, "A real-time parametric stiffness observer for VSA devices," in *Proc. IEEE Int. Conf. on Robotics and Automation*, Shanghai, PRC, 2011 (this conference).
- [12] A. Jafari, N. G. Tsagarakis, B. Vanderborght, and D. G. Caldwell, "An intrinsically safe actuator with the ability to adjust the stiffness," in *7th IARP Work. on Technical Challenges for Dependable Robots in Human Environments (DRHE 2010)*, Toulouse, F, 2010.
- [13] A. De Luca and R. Mattone, "Actuator failure detection and isolation using generalized momenta," in *Proc. IEEE Int. Conf. on Robotics and Automation*, 2003, pp. 634–639.
- [14] L. Le Tien, A. Albu-Schäffer, A. De Luca, and G. Hirzinger, "Friction observer and compensation for control of robots with joint torque measurements," in *Proc. IEEE Int. Conf. on Intelligent Robots and Systems*, 2008, pp. 3789–3795.
- [15] S. Haddadin, A. Albu-Schäffer, A. De Luca, and G. Hirzinger, "Collision detection and reaction: A contribution to safe physical human-robot interaction," in *Proc. IEEE/RSJ Int. Conf. on Intelligent Robots and Systems*, 2008, pp. 3356–3363.
- [16] R. Schiavi, G. Grioli, S. Sen, and A. Bicchi, "VSA-II: A novel prototype of variable stiffness actuator for safe and performing robots interacting with humans," in *Proc. IEEE Int. Conf. on Robotics and Automation*, 2008, pp. 2171–2176.
- [17] S. Wolf and G. Hirzinger, "A new variable stiffness design: Matching requirements of the next robot generation," in *Proc. IEEE Int. Conf. on Robotics and Automation*, 2008, pp. 1741–1746.
- [18] M. G. Catalano, R. Schiavi, and A. Bicchi, "Design of variable stiffness actuators mechanisms based on enumeration and analysis of performance," in *Proc. IEEE Int. Conf. on Robotics and Automation*, 2010, pp. 3285–3291.